JOURNAL OF VIROLOGY, Mar. 2006, p. 2506–2514 Vol. 80, No. 5
0022-538X/06/$08.00+0 doi:10.1128/JVI.80.5.2506–2514.2006

Preferential Infection of Mature Dendritic Cells by Mouse Hepatitis Virus Strain JHM

Haixia Zhou[1] and Stanley Perlman[1,2]*

Departments of Microbiology[1] and Pediatrics,[2] University of Iowa, Iowa City, Iowa 52242

Received 15 September 2005/Accepted 14 December 2005

Mouse hepatitis virus strain JHM (MHV-JHM) causes acute encephalitis and acute and chronic demyelinating diseases in mice. Dendritic cells (DCs) are key cells in the initiation of innate and adaptive immune responses, and infection of these cells could potentially contribute to a dysregulated immune response; consistent with this, recent results suggest that DCs are readily infected by another strain of mouse hepatitis virus, the A59 strain (MHV-A59). Herein, we show that the JHM strain also productively infected DCs. Moreover, mature DCs were at least 10 times more susceptible than immature DCs to infection with MHV-JHM. DC function was impaired after MHV-JHM infection, resulting in decreased stimulation of CD8 T cells in vitro. Preferential infection of mature DCs was not due to differential expression of the MHV-JHM receptor CEACAM-1a on mature or immature cells or to differences in apoptosis. Although we could not detect infected DCs in vivo, both $CD8^+$ and $CD11b^+$ splenic DCs were susceptible to infection with MHV-JHM directly ex vivo. This preferential infection of mature DCs may inhibit the development of an efficient immune response to the virus.

Several strains of mouse hepatitis virus (MHV), including the JHM and A59 strains, cause acute encephalitis and acute and chronic demyelinating diseases in mice (42). The adaptive immune response to murine coronaviruses has been partially characterized. Robust CD4 and CD8 T-cell responses to viral antigens have been detected in mice infected with most strains of MHV-JHM or MHV-A59 (34, 37, 43). An antivirus antibody response is also present in infected mice and is critical for preventing virus recrudescence (36). These results suggest that presentation of viral antigen to naïve T cells, a process that involves professional antigen-presenting cells such as DCs, is effective. Other studies, however, suggest that the anti-MHV CD8 T-cell response was not optimal in MHV-JHM-infected mice and was diminished compared to that observed in mice infected with the MHV-A59 strain (37). Although not examined, these effects may have resulted from suboptimal DC function.

DCs are critical in the host immune response to viral pathogens. DCs include several subsets based on phenotypic markers (CD11b, CD8, B220, Ly-6C). $CD8^+$ DCs are considered most important for T-cell cross-priming (8), whereas plasmacytoid DCs express large amounts of alpha/beta interferons (IFN-α/β) in response to viral infections (reviewed in reference 6). Viruses have developed strategies to depress the function of these cells. Some viruses impair DC function in vitro (2, 22, 26, 31), but only a few studies have examined the effect of viral infection in vivo. Certain immunosuppressive strains of lymphocytic choriomeningitis virus (LCMV) infect DCs in vivo, resulting, ultimately, in the loss of normal splenic architecture and in LCMV-specific CD8 T-cell exhaustion (12, 39). The immunosuppressive effect of LCMV involves, in part, the IFN-α/β-dependent suppression of DC expansion and maturation; measles virus activates the same pathway to inhibit DC maturation and proliferation in vivo (13). In an elegant set of studies, Andrews and colleagues showed that murine cytomegalovirus infected DCs in vivo and in vitro, resulting in the impaired upregulation of costimulatory molecules and diminished antigen processing. These defects, in turn, resulted in decreased ability to activate naïve T cells (1). While this effect on DC function was transient in infected mice, it most likely facilitated murine cytomegalovirus persistence.

Little is known about DC function in vivo after infection with MHV. Dendritic cells are readily infected by MHV-A59 and form syncytia in vitro (45). The primary host cell receptor for MHV is CEACAM-1a, a member of the carcinoembryonic antigen family (15). CEACAM-1a is expressed on DCs (20), and infection of DCs in vitro is CEACAM-1a dependent (45). After syncytium formation, DCs are unlikely to function normally. Development of the anti-MHV immune response would be compromised if large numbers of DCs were similarly infected in mice. Infection with virulent strains of MHV-JHM may have a more profound effect on the innate and adaptive immune responses than MHV-A59 (37). Also, there is an apparent contradiction between the relative ease with which DCs are infected in vitro and the robustness of the T-cell response in vivo. For both of these reasons, we assessed the extent to which DCs are infected by MHV-JHM after culture and in mice. We also extended these analyses to mature and immature populations of DCs.

MATERIALS AND METHODS

Mice. Specific-pathogen-free 5- to 8-week-old C57BL/6 (B6) mice (National Cancer Institute, Bethesda, MD) were used in most studies. Mice were inoculated intranasally with 6×10^4 PFU or intraperitoneally with 0.5×10^6 to 1.0×10^6 PFU of virus. P14 mice, transgenic for a T-cell receptor that recognizes the gp33 peptide from the LCMV glycoprotein, were provided by J. Harty (University of Iowa, Iowa City, IA).

* Corresponding author. Mailing address: Department of Pediatrics, University of Iowa, Medical Laboratories 2042, Iowa City, IA 52242. Phone: (319) 335-8549. Fax: (319) 335-8991. E-mail: Stanley-Perlman@uiowa.edu.

Virus. Recombinant and nonrecombinant MHV-JHM (MHV-JHM.IA [29], called MHV-JHM herein) were grown in 17Cl-1 cells and titers were determined on HeLa-MHVR cells as previously described (32). HeLa-MHVR cells express CEACAM-1a, the host cell receptor for MHV (15). In all experiments in which virus titers were measured, cells and supernatants were combined prior to titer measurement. Recombinant A59.GFP (rA59.GFP) was kindly provided by K. MacNamara and S. Weiss (University of Pennsylvania, Philadelphia, PA) (7).

Construction of rJHM.GFP. Targeted recombination was used as described previously to generate recombinant JHM virus expressing green fluorescent protein (rJHM.GFP) (21, 30) (see Fig. 1C). The primers for producing a GFP PCR product were CCCTGCAGGAAAGACAGAAAATCTAAACAATTTAT AGCATTTTAGTTGCTACTTTGCTCCTCTAGAGGGCAGCAGAAGTAGT TATGGTGAGCAAGGGCGAG (forward) and CCAGTCACGCGTATGGTA TCCGCCGCTTATGTACAGCTCGTC (reverse). Donor RNAs were transcribed using T7 polymerase and transfected into feline cells (AK-D) previously infected with feline MHV-JHM (fMHV-JHM), a recombinant MHV strain, encoding the feline surface (S) glycoprotein. fMHV-JHM does not infect murine cells, but recombinant virus expressing the MHV S protein does, allowing for the efficient selection of recombinant virus on 17Cl-1 murine cells. GFP expression after infection was confirmed by fluorescence microscopy.

Generation and infection of BM-derived DCs. Bone marrow (BM)-derived DCs were generated as previously described by Hamilton et al. and Inaba et al., with minor modification (14, 18). Briefly, red blood cell-depleted B6 BM cells were subjected to complement depletion after incubation with one of the following monoclonal antibodies (MAbs) as hybridoma supernatants: 3.168 (anti-CD8), RL172 (anti-CD4), or RA3-3A1/6.1 (anti-B220/CD45R) (kindly provided by M. Dailey and J. Harty, University of Iowa). Cells remaining after depletion were plated at a density of 1×10^6/ml in RP10 (RPMI with 10% fetal calf serum, 1.0 mM HEPES, 0.2 mM L-glutamine, 0.05 mM gentamicin sulfate, 1% penicillin-streptomycin, 1 mM sodium pyruvate, and 0.02 mM 2-mercaptoethanol) supplemented with 1,000 U/ml recombinant granulocyte-macrophage colony-stimulating factor (BD Pharmingen, San Diego, CA) and 25 U/ml recombinant interleukin-4 (PeproTech, Rocky Hill, NJ). Cells were incubated for 6 to 7 days with 75% medium replacement every 2 days. In some experiments, $CD11c^+$ cells were selected. For this purpose, cells were incubated sequentially with phycoerythrin (PE)-conjugated anti-CD11c antibody (BD Pharmingen) and anti-PE magnetic beads (Miltenyi Biotec, Cologne, Germany) or, alternatively, with biotin-conjugated anti-CD11c antibody (BD Pharmingen) and streptavidin magnetic beads (Miltenyi Biotec). $CD11c^+$ DCs were isolated using a Miltenyi autoMACS magnetic cell sorter (Miltenyi Biotec). The purity of isolated DCs was confirmed by fluorescence-activated cell sorter (FACS) analysis.

After 6 to 7 days in culture, DCs were infected with MHV-JHM or rJHM.GFP at a multiplicity of infection (MOI) of 1, except as noted below. In some experiments, DCs were infected with rA59.GFP.

Preparation of splenic DCs. Spleens were harvested and injected with 500 μl collagenase (0.395 mg/ml). After 30 min of incubation at 37°C, a single-cell suspension was prepared as previously described (47). In some instances, $CD11c^+$ cells were selected as described above. Cells were infected at an MOI of 10.

Viral growth kinetics in DCs. BM-derived DCs were harvested after 6 to 7 days in culture and infected with MHV-JHM or rJHM.GFP. After 30 min, cells were washed twice with phosphate-buffered saline (PBS) and harvested at the times indicated below. Virus titers were determined on HeLa-MHVR cells by plaque assay.

Immunofluorescence assays. BM-derived DCs infected with MHV-JHM were fixed in methanol at 7 to 9 h postinfection (p.i.). Cells were reacted with biotin-conjugated anti-CD11c MAb (BD Pharmingen) and anti-nucleocapsid (N) MAb (MAb 5B188.2; kindly provided by M. Buchmeier, The Scripps Research Institute, La Jolla, CA). Positive cells were identified using a tyramide signal amplification Cy3 kit (PerkinElmer, Boston, MA) and fluorescein isothiocyanate (FITC)-conjugated donkey anti-mouse antibody (Jackson Immunoresearch Laboratories, West Grove, PA), followed by confocal microscopy. Nuclei were detected with TO-PRO-3 (Molecular Probes, Eugene, Oregon).

In other experiments, frozen sections were prepared from brains harvested 5 days after intranasal inoculation with rJHM.GFP and fixed in paraformaldehyde. Sections were reacted with anti-N MAb, followed by Cy3-conjugated donkey anti-mouse antibody (Jackson Immunoresearch Laboratories).

Flow cytometric analysis and sorting. Antibodies used for phenotyping cells were PE-conjugated anti-CD11c, FITC, or biotinylated anti-CD86; FITC, PE, or biotinylated anti-B220; FITC-, PE-, or PE-Cy7-conjugated anti-CD8; FITC- or PerCP-conjugated CD11b (BD Pharmingen); and biotinylated anti-CEACAM-1a (kindly provided by K. Holmes, University of Colorado, Denver, CO). Biotinylated antibodies were detected with streptavidin-allophycocyanin (SA-APC; Molecular Probes) or SA-PerCP (BD Pharmingen). Samples were analyzed on a Becton Dickinson LSR II or FACScan flow cytometer (BD Biosciences, Mountain View, CA). $CD11c^+$ $CD86^{hi}$ and $CD11c^+$ $CD86^{lo}$ cells were sorted using a DIVA flow cytometer (BD Biosciences).

T-cell proliferation assay. BM-derived DCs were either mock infected or infected with MHV-JHM (MOI of 100) for 0, 2, 5, or 8 h before pulsing with 1 μM gp33 peptide for 1 h. Cells were harvested and washed with medium two times to remove soluble peptide. $CD8^+$ T cells were isolated by negative selection from the spleens of P14-Tg mice by using magnetic beads (Miltenyi Biotec). CFSE (5- and 6-carboxyfluorescein diacetate succinimidyl ester, 10 μM; Molecular Probes)-labeled P14-Tg $CD8^+$ T cells were then cocultured with the peptide-pulsed DCs at a DC/T-cell ratio of 1:100 or 1:500 at 37°C for 3 days in 96-well plates. Proliferation of T cells was then measured by flow cytometry. The division index is the average number of divisions calculated from the FACS data. In some experiments, T-cell apoptosis was assayed as described below.

Growth of MHV-JHM in cells treated with protease inhibitors. L929 cells or BM-derived DCs were preincubated for 4 h in medium that contained 0 to 100 μM CA074 (Sigma) or 0 to 10 μM FYdmk [Z-Phe-Tyr(t-Bu)-diazomethyl ketone; Calbiochem, La Jolla, CA]. The medium was removed, and cells were infected with MHV-JHM at an MOI of 1. After 30 min of incubation, cells were washed twice with PBS and then cultured with fresh medium supplemented with CA074 or FYdmk for 20 h. Viruses were titered on HeLa-MHVR cells by plaque assay.

Apoptosis assay. rJHM.GFP-infected, BM-derived DCs were harvested at 9 h p.i. and stained with PE-conjugated anti-CD11c and biotinylated annexin V (BD Pharmingen), followed by propidium iodide (PI; BD Pharmingen) and SA-APC staining. In other experiments, MHV-JHM-infected DCs were stained with PE-conjugated anti-CD11c, biotinylated annexin V, and FITC-conjugated anti-CD86 MAbs, followed by SA-APC.

IFN bioassay. Levels of IFN were measured using a bioassay based on the inhibition of vesicular stomatitis virus (VSV) growth in L929 cells. DCs were infected with MHV-JHM at an MOI of 1. Supernatants were harvested, and MHV-JHM was UV inactivated. L929 cells infected with 1,000 PFU VSV were treated with dilutions of supernatants or recombinant murine IFN-β (PBL Biomedical Laboratories, Piscataway, NJ) at 30 min p.i. Titers of VSV were determined on Vero cells. IFN levels were calculated based on the standard curves generated with recombinant IFN-β. To verify production of IFN by DCs, samples were treated with 25 μg/ml poly(I · C) (Invivogen, San Diego, CA) or 1 μg/ml lipopolysaccharide (LPS; Sigma, St. Louis, MO) and supernatants were assayed.

Sensitivity to IFN-β. The relative sensitivity of MHV-JHM to IFN-β was measured by treating DCs with serial dilutions of IFN-β for 24 h prior to infection with MHV-JHM. After infection, the same concentrations of IFN-β were added to the culture. In some experiments, infected DCs were treated only with serial dilutions of IFN-β 30 min after infection. MHV was titered on HeLa-MHVR cells. As a control, VSV-infected L929 cells were treated with IFN-β and virus titered on Vero cells.

RESULTS

MHV-JHM productively infects DCs. Initial experiments were directed at examining the ability of MHV-JHM to infect DCs after in vitro culture. For this purpose, we cultured DCs from murine BM as previously described (14, 18). Culture in the presence of interleukin-4/granulocyte-macrophage colony-stimulating factor results in the preferential outgrowth of myeloid DCs ($CD11b^+$ $CD11c^+$). After infection with MHV-JHM (MOI of 1), viral antigen was detected in infected, but not uninfected, cells by 7 h p.i. Virus-induced syncytium formation was apparent by 7 to 9 h p.i. Many, but not all, of the infected cells expressed the DC marker CD11c (Fig. 1A). To confirm that $CD11c^+$ cells were directly infected by the virus and not merely incorporated into syncytia initiated by other infected cells in the culture, we selected $CD11c^+$ cells by using magnetic beads prior to MHV-JHM infection. These cells were also infected by MHV-JHM (Fig. 1B). Infection with MHV-A59 was productive (45). Infection with MHV-JHM was also

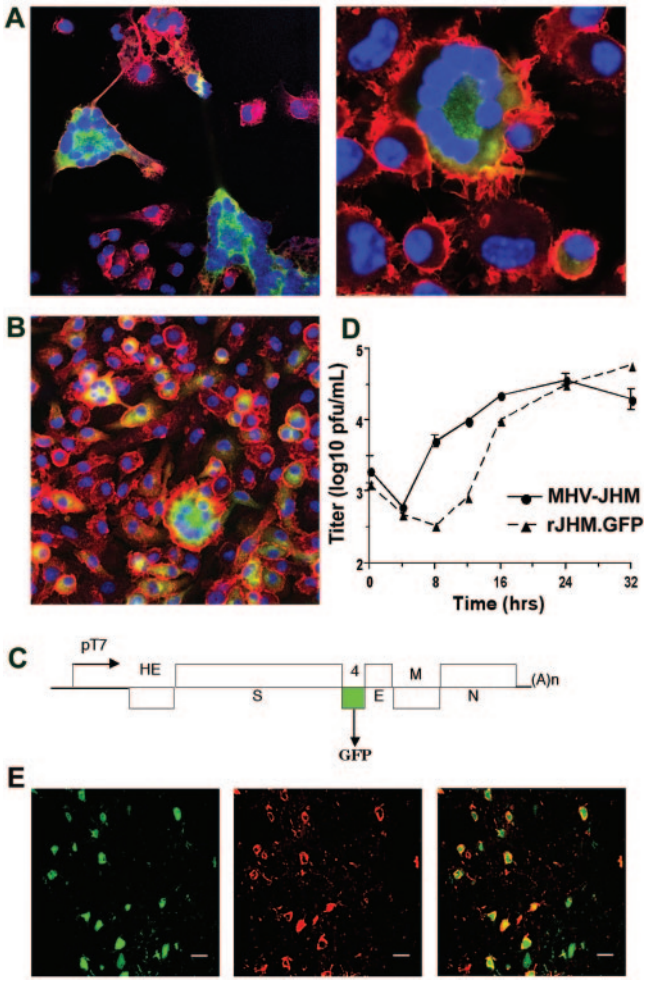

FIG. 1. MHV-JHM and rJHM.GFP productively replicate in BM-derived DCs. DCs were harvested from the bone marrow of naïve B6 mice and prepared as described in Materials and Methods. (A) After 6 to 7 days in culture, cells were infected with MHV-JHM at an MOI of 1 and fixed at 7 to 9 h p.i. Cells were stained for CD11c (red) and N protein (green). Nuclei were labeled with TO-PRO-3 (blue). Original magnifications: left, ×40; right, ×100. (B) DC cultures were enriched for $CD11c^+$ cells by using magnetic beads prior to infection with MHV-JHM. Cells were stained as described for panel A. Initial magnification, ×38. (C) A recombinant MHV-JHM expressing GFP was engineered as described in Materials and Methods, with GFP inserted into gene 4 (rJHM.GFP). HE, hemagglutinin-esterase; E, small membrane protein; M, transmembrane protein. (D) BM-derived DCs were infected with MHV-JHM or rJHM.GFP at an MOI of 1, and samples were harvested in triplicate for titers at the indicated times. Virus titers were determined by plaque assay on HeLa-MHVR cells. A representative example of three independent experiments is shown in the figure. (E) Mice were inoculated with 6×10^4 PFU rJHM.GFP intranasally. Brains were harvested and analyzed for MHV-JHM N antigen (red) and GFP expression (green). Original magnification, ×40. Scale bar, 20 μM.

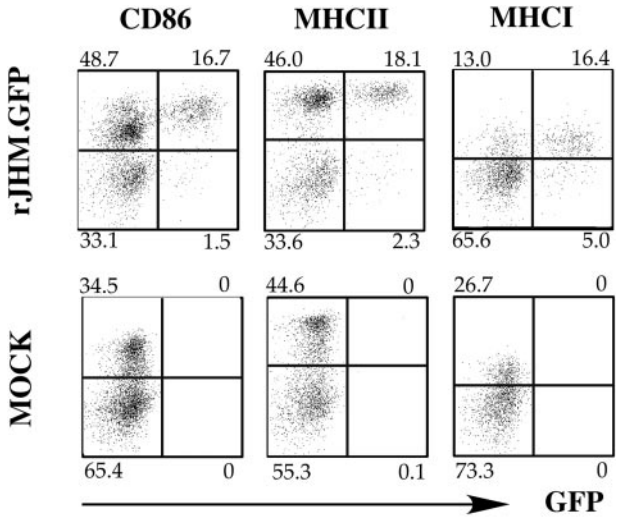

FIG. 2. rJHM.GFP-infected DCs are MHC class I/II^{hi} and $CD86^{hi}$. DCs were infected with rJHM.GFP at an MOI of 10. After 9 h, cells were harvested and the expression of CD11c, MHC class I, MHC class II, and CD86 molecules, as well as GFP, was assessed by FACS analysis. Shown are data for samples after gating on $CD11c^+$ cells. The percentage of infected cells was determined by GFP expression. The data for the experiment shown are representative of 10 independent experiments.

productive with newly produced infectious virus detected as early as 8 h p.i. (Fig. 1D). Virus titers were maximal at 24 h p.i.

MHV-JHM preferentially infects $CD86^{hi}$ and MHC class I/II^{hi} mature DCs. Immature DCs phagocytose antigen and migrate to lymphoid organs. After maturation, as evidenced by costimulatory molecule and major histocompatibility complex (MHC) class I/II antigen upregulation, DCs are able to present antigen to naïve T cells. To determine whether mature or immature DCs were preferentially infected with MHV-JHM, we infected unfractionated BM-derived DCs with MHV-JHM and analyzed cells by FACS analysis. To simplify analyses, we developed a recombinant MHV-JHM virus that expressed GFP (rJHM.GFP), as described in Materials and Methods (Fig. 1C). GFP was introduced into gene 4 by using targeted recombination, since we and others have shown that the gene 4 protein is not essential for viral growth in tissue culture cells or for the induction of acute encephalitis (30, 49). rJHM.GFP replicates with slower kinetics in tissue culture cells but causes acute encephalitis with approximately the same kinetics as nonrecombinant MHV-JHM (Fig. 1D and data not shown). This difference in the in vitro growth kinetics was reported previously for all recombinant MHV-JHM and does not specifically reflect the presence of GFP (30). After 10 passages of rJHM.GFP in vitro, more than 90% of infected cells still expressed GFP. Also, after intranasal inoculation of B6 mice, nearly all infected cells in the brain, as detected by N protein expression, were GFP^+ (Fig. 1E). Similar results were obtained when virus harvested from the central nervous system was grown in tissue culture cells and assayed for GFP expression (data not shown).

When DCs were infected with this virus and stained for CD11c, MHC class I/II, and CD86, the majority of infected $CD11c^+$ cells were MHC class I/II^{hi} and $CD86^{hi}$, consistent with a mature phenotype (Fig. 2). Cells were analyzed at 9 h p.i. to maximize the detection of infected cells but minimize the percentage of cells in syncytia; syncytia are not easily detectable by cell sorter analysis. These results also suggested that MHV-JHM infection does not result in the downregulation of costimulatory molecules, as occurs in other viral infec-

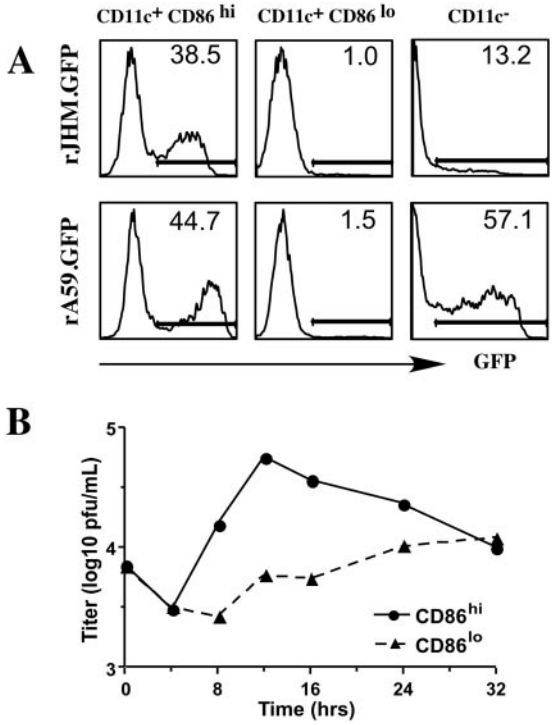

FIG. 3. rJHM.GFP and rA59.GFP preferentially infect mature DCs. (A) $CD86^{hi}$ or $CD86^{lo}$ DCs and $CD11c^{-}$ DC precursors in the culture were separated using a flow cytometer prior to infection with rJHM.GFP or rA59.GFP (MOI of 10). Cells were harvested at 9 h p.i., and the percentage of GFP^{+} cells in each population was assessed by FACS analysis. (B) $CD86^{hi}$ or $CD86^{lo}$ DCs were infected with MHV-JHM at an MOI of 10. Virus titers were measured at the indicated times by plaque assay. The experiments shown in each panel are representative samples from three independent experiments.

tions (1). While these results show that infected cells are mature DCs, MHV-JHM either may directly infect mature DCs or may infect immature DCs and induce their subsequent maturation. To distinguish between these possibilities, we separated $CD86^{hi}$ and $CD86^{lo}$ DCs by flow cytometric sorting prior to infection with rJHM.GFP. As shown for rJHM.GFP-infected cells at 9 h p.i., $CD86^{hi}$ cells were preferentially infected by the virus (Fig. 3A). In these analyses, cells were infected at an MOI of 10, and the fraction of $CD86^{hi}$ cells that were GFP^{+} was at least 10 times higher than that of $CD86^{lo}$ cells. However, even by 9 h p.i., some syncytia were present in both populations. To eliminate the possibility that infected immature DCs preferentially formed syncytia and were therefore excluded from the FACS analysis, we quantified the proportion of GFP^{+} cells by fluorescence microscopy. Again, the percentage of GFP^{+} cells was more than 10 times higher in $CD86^{hi}$ (32.6% ± 3.7%) than in $CD86^{lo}$ (2.1% ± 1.5%) DCs after infection at an MOI of 10. Infection of both cell types was productive, although only low levels of infectious virus were released from $CD86^{lo}$ cells (Fig. 3B). Virus titers diminished at later times p.i. in the $CD86^{hi}$ cultures, probably as a consequence of virus-mediated cell death.

Of note, rA59.GFP also preferentially infects mature DCs (Fig. 3A). Both viruses also infect $CD11c^{-}$ cells within the dendritic cell culture, but rA59.GFP infects a higher percentage of these cells than does rJHM.GFP (Fig. 3A).

DC function is impaired after infection. While cells in syncytia are unlikely to present antigen efficiently, it is possible that MHV-JHM infection decreases antigen presentation by DCs even at early times p.i. To examine this possibility, MHV-JHM-infected BM-derived DCs were pulsed with gp33 peptide and incubated for 3 days with CFSE-labeled P14-Tg CD8 T cells at a DC/T-cell ratio of 1:100 or 1:500. In these assays, only a short period of exposure of T cells to DCs is required for their maximal proliferation (46). Mock-infected DCs stimulated P14-Tg CD8 T cells to proliferate (Fig. 4A). However, even by 3 h p.i., DCs in infected cultures were impaired in their ability to prime naïve T cells. Both the percentage of divided cells and the division index were decreased by 25 to 40% at 3 h p.i. This effect was more noticeable by 6 h, although only a few syncytia were observed in the cultures at this time. This lack of proliferation of T cells was not a consequence of the induction of apoptosis or cell death by the infected DCs because we detected no increases in annexin V or PI staining in the cocultured T cells (Fig. 4B). Another possibility is that T cells, known to upregulate CEACAM-1a expression after activation (28), become infected in the cocultures. However, we detected no GFP^{+} T cells when P14-Tg T cells were incubated with rJHM.GFP-infected DCs or when naïve T cells were activated with phorbol 12-myristate 13-acetate and ionomycin prior to infection with rJHM.GFP (data not shown).

Preferential infection of $CD86^{hi}$ cells does not correlate with higher levels of CEACAM-1a surface expression or increased apoptosis. One explanation for the difference in infection rate between mature and immature DCs is that CEACAM-1a, the MHV receptor, is expressed at higher levels on $CD86^{hi}$ cells. To assess surface levels of CEACAM-1a, we incubated unfractionated $CD11c^{+}$ DCs with anti-CEACAM-1a MAb. As shown in Fig. 5, similar levels of CEACAM-1a were expressed on $CD86^{hi}$ and $CD86^{lo}$ cells after flow cytometric analysis. These results agree with a previous report showing that CEACAM-1a surface expression was not increased after DC maturation (20).

Another possible explanation for the observed difference was that MHV-JHM preferentially induced apoptosis in $CD86^{lo}$ cells, thereby inhibiting virus replication prior to GFP expression. MHV has been shown to induce apoptosis in infected fibroblasts, although signs of apoptosis were not detected until 16 to 20 h p.i. (5). However, we observed that only a small percentage of infected or uninfected cells in rJHM.GFP-infected DC cultures were apoptotic (annexin V^{+} PI^{-}) (Fig. 6A). In addition, there was no difference in the proportion of $CD86^{hi}$ or $CD86^{lo}$ cells that underwent apoptosis when MHV-JHM-infected and uninfected cultures were compared at 9 h p.i. (Fig. 6B).

Viral growth is not affected by treatment with cathepsin B and cathepsin L inhibitors. Entry of severe acute respiratory syndrome coronavirus (SARS-CoV) was recently shown to require exposure to cathepsin L in the endosomes (41). Furthermore, cathepsin L is upregulated in DCs upon maturation (44). Therefore, to determine if this upregulated expression of cathepsin L in mature DCs contributed to their increased susceptibility to MHV-JHM, we treated cells with FYdmk, an inhibitor of cathepsin L (40). Initially, we treated L929 cells with the inhibitor at a range of concentrations, 0 to 10 μM.

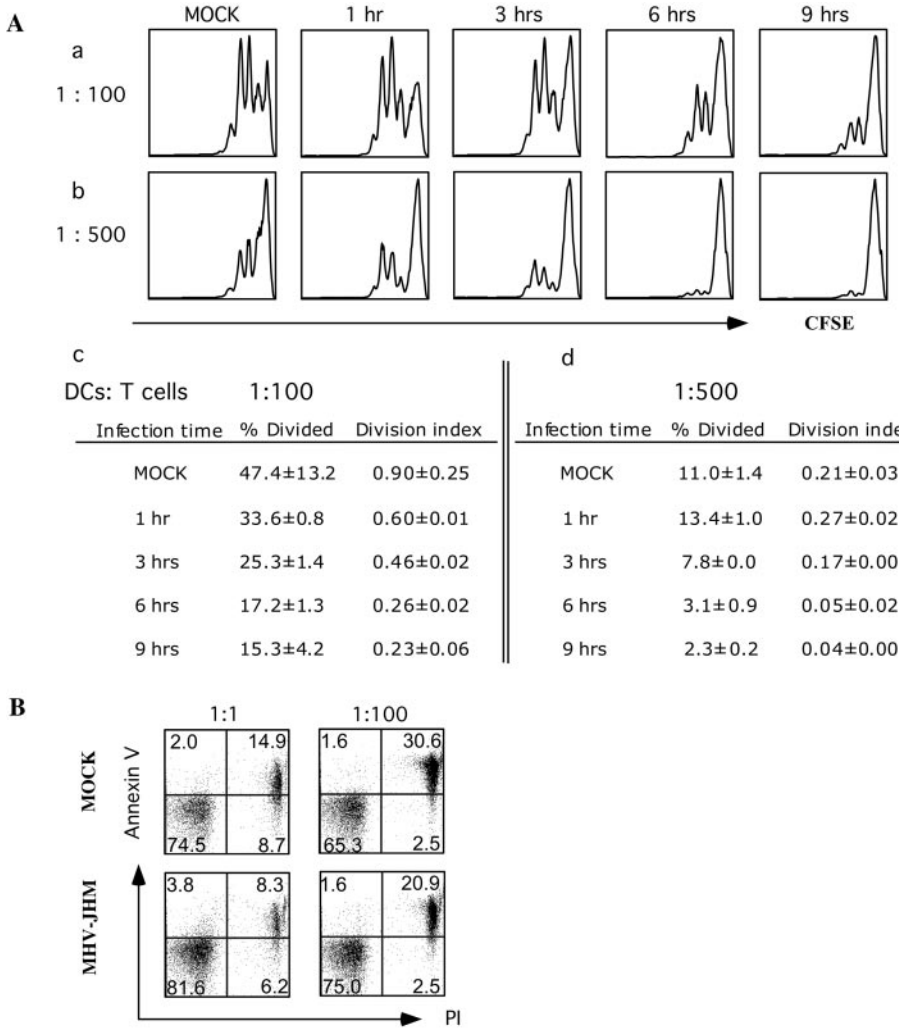

FIG. 4. Infection of DCs with MHV-JHM impairs their ability to induce T-cell proliferation. (A) BM-derived DCs were infected with MHV-JHM for 1, 3, 6, or 9 h at an MOI of 100 or mock infected. Following pulsing with gp33 peptide for 1 h, mock- or MHV-JHM-infected DCs were added to CFSE-labeled P14-Tg $CD8^+$ T cells and incubated for 3 days. Ratios of 1:100 (panels a and c) and 1:500 (panels b and d) DCs to T cells are shown. (a and b) T-cell proliferation was analyzed by FACS analysis. (c and d) The percentage of the total number of cells that have divided (% Divided), as well as the average number of divisions the cell population has undergone (Division index), was calculated. Compared to mock-infected DCs and DCs harvested at 1 h p.i., the percentage of divided cells and division index in DCs harvested at 3, 6, or 9 h are significantly different for both DC/T-cell ratios shown in the figure ($P < 0.05$). The data are representative of three independent experiments. (B) To determine whether infected DCs induced apoptosis of T cells, DCs were infected with MHV-JHM for 6 h, pulsed with gp33 peptide, and added to P14-Tg $CD8^+$ T cells at a ratio of 1:1 or 1:100. After incubation for 24 h, cells were harvested and stained with annexin V and PI.

SARS-CoV entry is inhibited nearly completely by 1 μM Z-III-FMK, another cathepsin L inhibitor (41). However, we detected no significant effect on MHV-JHM growth in L929 cells. Similarly, MHV-JHM growth in DCs was not significantly changed by treatment with FYdmk (Fig. 7). Cathepsin B is required for Ebola virus entry (4). We observed no effect on MHV-JHM growth in L929 cells after treatment with CA074 (27), a specific cathepsin B inhibitor (data not shown).

Infection of DCs in vivo and directly ex vivo. These results show that MHV-JHM readily infects DCs in vitro and causes syncytium formation, but nothing is known about the infection of DCs in animals by any strain of MHV. To determine the extent of infection of DCs in vivo, we inoculated mice intraperitoneally with 0.5×10^6 to 1.0×10^6 PFU of rJHM.GFP and analyzed spleens and mesenteric lymph nodes at 12, 24, and 48 h p.i. by FACS analysis for GFP^+ cells. We detected no MHV-JHM-positive DCs in the spleen or mesenteric lymph nodes by this approach. Furthermore, MHV-JHM infection did not induce any changes in the relative proportions of different DC subsets or in their maturation status in these organs ($CD8^+$ $CD11b^-$ $CD11c^+$ versus $CD8^-$ $CD11b^+$ $CD11c^+$ or $CD86^{hi}$ $CD11c^+$ versus $CD86^{lo}$ $CD11c^+$) (data not shown). To increase the likelihood of detecting infected DCs, we selected $CD11c^+$ cells by magnetic bead sorting from the spleens of rJHM.GFP-infected mice. When these cells were directly examined by fluorescence microscopy, we still could not detect any GFP^+ cells. In another approach, we examined cervical lymph nodes for GFP^+ cells after intranasal inoculation of rJHM.GFP; these mice developed acute encephalitis by 6 to 7 days p.i. However, we detected no GFP^+ cells at 12, 24, or 48 h

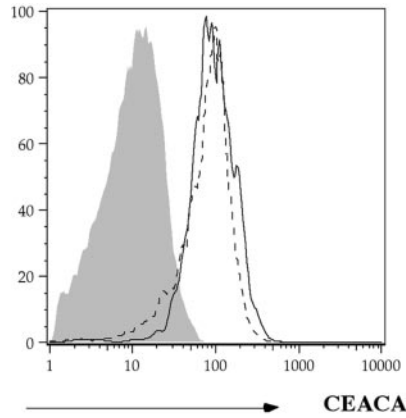

FIG. 5. CEACAM-1a expression levels on mature and immature DCs are equivalent. DCs were stained sequentially with biotinylated anti-CEACAM-1a MAb and SA-PerCP and analyzed by FACS analysis. Shaded, immunoglobulin control; solid line, CD86^{hi} DCs; dashed line, CD86^{lo} DCs.

p.i. These results are not due to a loss of GFP expression after passage in vivo because GFP was readily detected in nearly all infected cells in the brain after intranasal inoculation (Fig. 1E).

It is possible that DCs are infected in vivo but that infected cells are rapidly cleared. To address this possibility, we infected

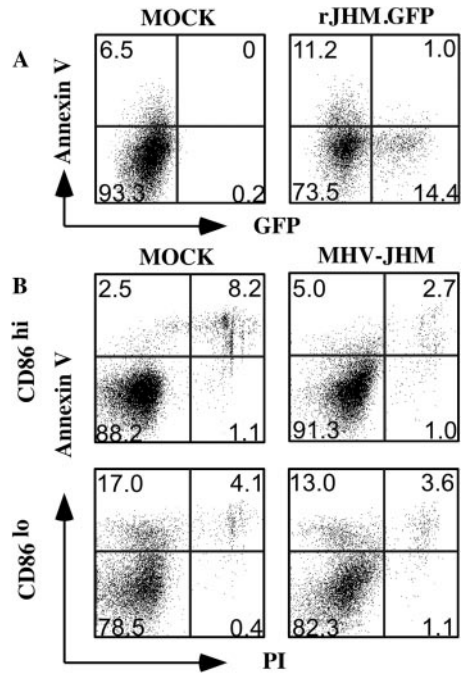

FIG. 6. Infection with MHV-JHM does not induce apoptosis in DCs. (A) BM-derived DCs were infected with rJHM.GFP (MOI = 10). Cells were harvested and stained with annexin V and PI at 9 h p.i. PI-negative cells are shown in the figure. Only a low percentage of infected (GFP$^+$) or uninfected (GFP$^-$) cells underwent apoptosis (annexin V$^+$) within the infected culture (right hand panel). (B) CD86^{hi} and CD86^{lo} DCs were sorted using a flow cytometer and infected with MHV-JHM (MOI = 10). MHV-JHM infection did not induce apoptosis in either CD86^{hi} or CD86^{lo} DC cultures compared to mock-infected cultures at 9 h p.i.

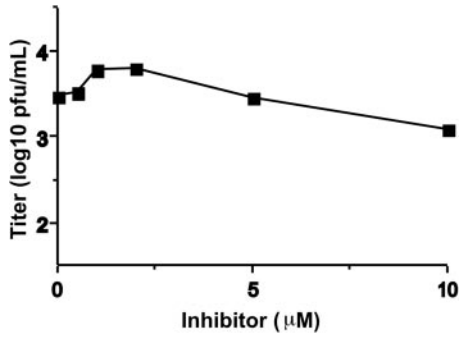

FIG. 7. MHV-JHM replication in DCs is not dependent on cathepsin L. DCs were treated with increasing doses of the cathepsin L inhibitor, FYdmk, 4 h prior to infection with MHV-JHM. After incubation for 20 h, viruses were harvested and titers were determined on HeLa-MHVR cells.

splenic DCs harvested from naïve mice directly ex vivo. Initially, unfractionated splenic cells were infected with rJHM. GFP and analyzed by FACS analysis at 9 h p.i. Approximately 1 to 2% of CD11c$^+$ cells were GFP$^+$ (data not shown), as were 1% of B220$^+$ CD11c$^-$ B cells (Fig. 8A). B cells express high levels of the MHV receptor CEACAM-1a, but others have previously shown that they are not readily infected by MHV (25). DCs comprise less than 1% of splenocytes, making FACS analyses of DC subpopulations within unfractionated spleen populations difficult. Therefore, we selected CD11c$^+$ cells by magnetic bead sorting and infected them with rJHM.GFP at an

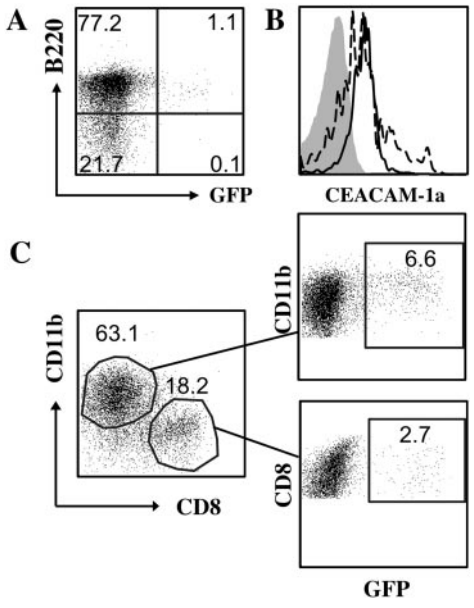

FIG. 8. Infection of splenic DCs and B cells directly ex vivo. (A) Spleen cells were harvested from naïve B6 mice and directly infected with rJHM.GFP (MOI of 1). A small percentage of B220$^+$ B cells were infected as showing by GFP expression. (B) CEACAM-1a expression levels were equivalent on CD8$^+$ CD11b$^-$ and CD8$^-$ CD11b$^+$ splenic DCs harvested from naïve mice. Shaded, immunoglobulin control; solid line, CD8$^-$ CD11b$^+$ DCs; dashed line, CD8$^+$ CD11b$^-$ DCs. (C) CD11c$^+$ cells were enriched using magnetic beads prior to infection with rJHM.GFP at an MOI of 10. Both CD8$^+$ and CD11b$^+$ DCs were susceptible to infection with the virus.

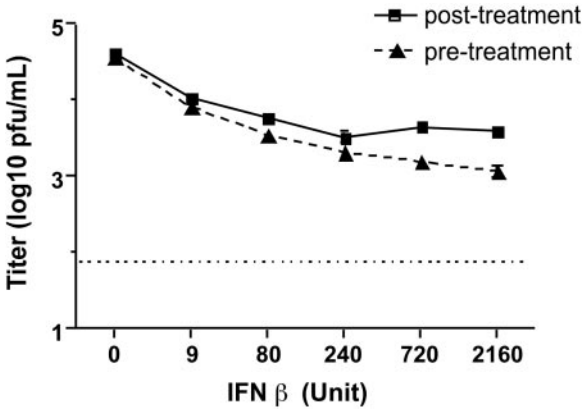

FIG. 9. MHV-JHM infection of DCs is modestly sensitive to IFN-β treatment. BM-derived DCs were treated with different concentrations of IFN-β prior to and after or only after infection with MHV-JHM (MOI = 1). Cells were harvested at 20 h p.i., and virus titers were determined by plaque assay. The dotted line shows the limit of detection of virus. One of three independent experiments is shown in the figure.

MOI of 10. The process of selection results in the activation of approximately 20% of DCs. Approximately 2 to 5% of total DCs were infected by the virus. Cells were also stained for CD8 and CD11b expression. As shown in Fig. 8C, both cell populations ($CD8^+$ $CD11b^-$ $CD11c^+$ and $CD8^-$ $CD11b^+$ $CD11c^+$) could be infected by rJHM.GFP. Of note, both subsets express CEACAM-1a at equivalent levels (Fig. 8B).

MHV-JHM does not induce interferon production in DCs and is modestly sensitive to IFN treatment. A key function of both plasmacytoid DCs and myeloid DCs is to produce IFN-α/β (9). MHV-infected fibroblasts do not express significant amounts of IFN and are only modestly sensitive to IFN-β treatment (11, 33). Consistent with these results, infection with MHV-JHM did not induce interferon production by DCs (<1 U) at 9 h or even at 20 h p.i., when more than 50% of the cells in the DC culture were infected and formed syncytia. In contrast, treatment with poly(I · C) or LPS for 20 h induced significant amounts of IFN [with poly(I · C), 148.6 ± 20.0 U; with LPS, 20.3 ± 0.7 U]. Replication of MHV-JHM in DCs was diminished only modestly when DCs were treated with murine IFN-β prior to and after infection, even after exposure to high doses. Even less inhibition was observed when cells were posttreated with IFN-β (Fig. 9). Thus, as in fibroblasts, MHV-JHM replication in DCs is only moderately inhibited by IFN-β treatment.

DISCUSSION

Our results show that MHV-JHM infects cultured BM-derived DCs, with extensive syncytium formation, but that DC infection in vivo is not easily detectable. Part of the explanation for this disparity between in vivo and in vitro infection is that MHV-JHM has a propensity to infect mature DCs whereas the vast majority of DCs in naïve or infected animals are immature. This results in a small percentage of the total DC population that is susceptible to infection with MHV-JHM. Other viruses also preferentially infect mature DCs. For example, mature blood-derived human DCs are infected at a higher level by respiratory syncytial virus than are immature cells (2). Although human cytomegalovirus preferentially infects immature blood-borne DCs, other results show that the virus also has a tropism for mature Langerhans cells (16). Some viruses infect mature DCs and downregulate surface expression of MHC class II and costimulatory molecules, thereby impairing T-cell activation (26). However, we did not observe downregulation of these molecules on MHV-JHM-infected cells (Fig. 2).

Our results suggest that MHV-JHM replicates more efficiently in mature DCs than in immature cells. The MHV receptor CEACAM-1a is expressed at equivalent levels on mature and immature DCs, suggesting that this difference does not occur at the level of initial binding to cells (Fig. 5). While MHV-A59, like MHV-JHM, preferentially infected mature DCs, we observed that $CD11c^-$ cells, which serve as precursors to DCs in these cultures, were 5 to 10 times more susceptible to MHV-A59 infection than MHV-JHM (Fig. 3A). This may occur because MHV-JHM appears to require a second host factor for the efficient infection of some cells. In previous studies, a difference in the ability of MHV-JHM and MHV-A59 to infect a set of cell lines derived from susceptible mice was observed, with MHV-JHM infecting some of these cells very inefficiently (48). Of note, MHV-JHM or MHV-A59 infection of even mature DCs is not very efficient in vitro, with only 70% of mature DCs infected by MHV-JHM at an MOI of 100 (data not shown).

While a second factor required for MHV-JHM infection of cells has not been identified, it is noteworthy that infection of cells by SARS-CoV is facilitated by the presence of one or more molecules in addition to angiotensin-converting enzyme 2, the primary receptor for the virus (23). In the case of SARS-CoV, the presence of either DC-SIGN or DC-SIGNR may enhance virus binding and subsequent entry (19, 24). As discussed above, recent data show that an endosomal (acid-pH-dependent) protease, cathepsin L, is required for the fusion of SARS-CoV (41). MHV-JHM fusion with the host cell membrane may also require a similar protease, and this might contribute to preferential infection of mature DCs. Our results show that cathepsins L and B are unlikely to be the proteases involved in MHV-JHM fusion. This may not be surprising because MHV-JHM, unlike SARS-CoV, undergoes a pH-independent fusion reaction to deliver infectious viral RNA into the cells (10).

Our results suggest a mechanism by which MHV-JHM may delay the onset of the immune response. Even 3 h after infection, exposure to MHV-JHM significantly reduced DCs' ability to stimulate the proliferation of antigen-specific CD8 T cells (Fig. 4A). Previous work showed that naïve T cells were nearly completely activated by as short an exposure as 2 h to peptide-labeled antigen-presenting cells (46). MHV-JHM did not induce syncytium formation or cell death in infected DCs until 6 to 7 h p.i., suggesting that a decrease in viable cell number did not account for the observation that DCs functioned suboptimally at 3 h p.i. We could not detect any MHV-JHM-induced downregulation of the costimulatory molecule CD86 or of MHC class I/II expression after infection (Fig. 2). This lack of downregulation of CD86 was also observed in purified cultures of $CD86^{hi}$ DCs after MHV-JHM infection (data not shown). Thus, the precise mechanism of MHV-JHM inhibition of DC function at early times p.i. remains to be investigated.

In terms of other components of the innate immune response, MHV-JHM did not induce IFN production, and virus replication was only modestly sensitive to IFN treatment in fibroblasts (11, 33) or DCs (Fig. 9). The lack of IFN-α/β production that we observed may also contribute to the relatively small amount of DC maturation that occurred in infected cultures (Fig. 2). Many RNA viruses, such as dengue virus, respiratory syncytial virus, measles, and parainfluenza virus type 3, induce maturation after in vitro infection of blood-derived human DCs or BM-derived murine DCs in a process that often involves IFN (2, 3, 13, 17, 35, 38).

Collectively, our results suggest that MHV-JHM hampers the initiation of the innate and adaptive antiviral immune responses by infecting mature DCs and inhibiting IFN production from these cells. Future work will be directed at determining the mechanism of the differential infection of mature and immature DCs.

ACKNOWLEDGMENTS

We thank John Harty for critical review of the manuscript and Lecia Pewe and Taeg Kim for helpful discussions.

This work was supported in part by grants from the NIH (RO1 NS36592) and the National Multiple Sclerosis Society (RG-2864).

REFERENCES

1. **Andrews, D. M., C. E. Andoniou, F. Granucci, P. Ricciardi-Castagnoli, and M. A. Degli-Esposti.** 2001. Infection of dendritic cells by murine cytomegalovirus induces functional paralysis. Nat. Immunol. **2:**1077–1084.
2. **Bartz, H., O. Turkel, S. Hoffjan, T. Rothoeft, A. Gonschorek, and U. Schauer.** 2003. Respiratory syncytial virus decreases the capacity of myeloid dendritic cells to induce interferon-gamma in naive T cells. Immunology **109:**49–57.
3. **Cella, M., M. Salio, Y. Sakakibara, H. Langen, I. Julkunen, and A. Lanzavecchia.** 1999. Maturation, activation, and protection of dendritic cells induced by double-stranded RNA. J. Exp. Med. **189:**821–829.
4. **Chandran, K., N. J. Sullivan, U. Felbor, S. P. Whelan, and J. M. Cunningham.** 2005. Endosomal proteolysis of the Ebola virus glycoprotein is necessary for infection. Science **308:**1643–1645.
5. **Chen, C. J., and S. Makino.** 2002. Murine coronavirus-induced apoptosis in 17Cl-1 cells involves a mitochondria-mediated pathway and its downstream caspase-8 activation and bid cleavage. Virology **302:**321–332.
6. **Colonna, M., G. Trinchieri, and Y. J. Liu.** 2004. Plasmacytoid dendritic cells in immunity. Nat. Immunol. **5:**1219–1226.
7. **Das Sarma, J., E. Scheen, S. H. Seo, M. Koval, and S. R. Weiss.** 2002. Enhanced green fluorescent protein expression may be used to monitor murine coronavirus spread in vitro and in the mouse central nervous system. J. Neurovirol. **8:**381–391.
8. **den Haan, J. M., S. M. Lehar, and M. J. Bevan.** 2000. CD8(+) but not CD8(−) dendritic cells cross-prime cytotoxic T cells in vivo. J. Exp. Med. **192:**1685–1696.
9. **Diebold, S. S., M. Montoya, H. Unger, L. Alexopoulou, P. Roy, L. E. Haswell, A. Al-Shamkhani, R. Flavell, P. Borrow, and C. Reis e Sousa.** 2003. Viral infection switches non-plasmacytoid dendritic cells into high interferon producers. Nature **424:**324–328.
10. **Gallagher, T. M., C. Escarmis, and M. J. Buchmeier.** 1991. Alteration of the pH dependence of coronavirus-induced cell fusion: effect of mutations in the spike glycoprotein. J. Virol. **65:**1916–1928.
11. **Garlinghouse, L. E., Jr., A. L. Smith, and T. Holford.** 1984. The biological relationship of mouse hepatitis virus (MHV) strains and interferon: in vitro induction and sensitivities. Arch. Virol. **82:**19–29.
12. **Hahm, B., N. Arbour, D. Naniche, D. Homann, M. Manchester, and M. B. Oldstone.** 2003. Measles virus infects and suppresses proliferation of T lymphocytes from transgenic mice bearing human signaling lymphocytic activation molecule. J. Virol. **77:**3505–3515.
13. **Hahm, B., M. J. Trifilo, E. I. Zuniga, and M. B. Oldstone.** 2005. Viruses evade the immune system through type I interferon-mediated STAT2-dependent, but STAT1-independent, signaling. Immunity **22:**247–257.
14. **Hamilton, S. E., B. B. Porter, K. A. Messingham, V. P. Badovinac, and J. T. Harty.** 2004. MHC class Ia-restricted memory T cells inhibit expansion of a nonprotective MHC class Ib (H2–M3)-restricted memory response. Nat. Immunol. **5:**159–168.
15. **Hemmila, E., C. Turbide, M. Olson, S. Jothy, K. V. Holmes, and N. Beauchemin.** 2004. *Ceacam1a*$^{-/-}$ mice are completely resistant to infection by murine coronavirus mouse hepatitis virus A59. J. Virol. **78:**10156–10165.
16. **Hertel, L., V. G. Lacaille, H. Strobl, E. D. Mellins, and E. S. Mocarski.** 2003. Susceptibility of immature and mature Langerhans cell-type dendritic cells to infection and immunomodulation by human cytomegalovirus. J. Virol. **77:**7563–7574.
17. **Ho, L. J., J. J. Wang, M. F. Shaio, C. L. Kao, D. M. Chang, S. W. Han, and J. H. Lai.** 2001. Infection of human dendritic cells by dengue virus causes cell maturation and cytokine production. J. Immunol. **166:**1499–1506.
18. **Inaba, K., M. Inaba, N. Romani, H. Aya, M. Deguchi, S. Ikehara, S. Muramatsu, and R. M. Steinman.** 1992. Generation of large numbers of dendritic cells from mouse bone marrow cultures supplemented with granulocyte/macrophage colony-stimulating factor. J. Exp. Med. **176:**1693–1702.
19. **Jeffers, S. A., S. M. Tusell, L. Gillim-Ross, E. M. Hemmila, J. E. Achenbach, G. J. Babcock, W. D. Thomas, Jr., L. B. Thackray, M. D. Young, R. J. Mason, D. M. Ambrosino, D. E. Wentworth, J. C. Demartini, and K. V. Holmes.** 2004. CD209L (L-SIGN) is a receptor for severe acute respiratory syndrome coronavirus. Proc. Natl. Acad. Sci. USA **101:**15748–15753.
20. **Kammerer, R., D. Stober, B. B. Singer, B. Obrink, and J. Reimann.** 2001. Carcinoembryonic antigen-related cell adhesion molecule 1 on murine dendritic cells is a potent regulator of T cell stimulation. J. Immunol. **166:**6537–6544.
21. **Kuo, L., G. J. Godeke, M. J. Raamsman, P. S. Masters, and P. J. Rottier.** 2000. Retargeting of coronavirus by substitution of the spike glycoprotein ectodomain: crossing the host cell species barrier. J. Virol. **74:**1393–1406.
22. **Larsson, M., A. S. Beignon, and N. Bhardwaj.** 2004. DC-virus interplay: a double edged sword. Semin. Immunol. **16:**147–161.
23. **Li, W., M. J. Moore, N. Vasilieva, J. Sui, S. K. Wong, M. A. Berne, M. Somasundaran, J. L. Sullivan, K. Luzuriaga, T. C. Greenough, H. Choe, and M. Farzan.** 2003. Angiotensin-converting enzyme 2 is a functional receptor for the SARS coronavirus. Nature **426:**450–454.
24. **Marzi, A., T. Gramberg, G. Simmons, P. Moller, A. J. Rennekamp, M. Krumbiegel, M. Geier, J. Eisemann, N. Turza, B. Saunier, A. Steinkasserer, S. Becker, P. Bates, H. Hofmann, and S. Pohlmann.** 2004. DC-SIGN and DC-SIGNR interact with the glycoprotein of Marburg virus and the S protein of severe acute respiratory syndrome coronavirus. J. Virol. **78:**12090–12095.
25. **Morales, S., B. Parra, C. Ramakrishna, D. M. Blau, and S. A. Stohlman.** 2001. B-cell-mediated lysis of cells infected with the neurotropic JHM strain of mouse hepatitis virus. Virology **286:**160–167.
26. **Morrow, G., B. Slobedman, A. L. Cunningham, and A. Abendroth.** 2003. Varicella-zoster virus productively infects mature dendritic cells and alters their immune function. J. Virol. **77:**4950–4959.
27. **Murata, M., S. Miyashita, C. Yokoo, M. Tamai, K. Hanada, K. Hatayama, T. Towatari, T. Nikawa, and N. Katunuma.** 1991. Novel epoxysuccinyl peptides. Selective inhibitors of cathepsin B, in vitro. FEBS Lett. **280:**307–310.
28. **Nakajima, A., H. Iijima, M. F. Neurath, T. Nagaishi, E. E. Nieuwenhuis, R. Raychowdhury, J. Glickman, D. M. Blau, S. Russell, K. V. Holmes, and R. S. Blumberg.** 2002. Activation-induced expression of carcinoembryonic antigen-cell adhesion molecule 1 regulates mouse T lymphocyte function. J. Immunol. **168:**1028–1035.
29. **Ontiveros, E., T. S. Kim, T. M. Gallagher, and S. Perlman.** 2003. Enhanced virulence mediated by the murine coronavirus, mouse hepatitis virus strain JHM, is associated with a glycine at residue 310 of the spike glycoprotein. J. Virol. **77:**10260–10269.
30. **Ontiveros, E., L. Kuo, P. S. Masters, and S. Perlman.** 2001. Inactivation of expression of gene 4 of mouse hepatitis virus strain JHM does not affect virulence in the murine CNS. Virology **290:**230–238.
31. **Palmer, D. R., P. Sun, C. Celluzzi, J. Bisbing, S. Pang, W. Sun, M. A. Marovich, and T. Burgess.** 2005. Differential effects of dengue virus on infected and bystander dendritic cells. J. Virol. **79:**2432–2439.
32. **Perlman, S., R. Schelper, E. Bolger, and D. Ries.** 1987. Late onset, symptomatic, demyelinating encephalomyelitis in mice infected with MHV-JHM in the presence of maternal antibody. Microb. Pathog. **2:**185–194.
33. **Pewe, L., H. Zhou, J. Netland, C. Tangadu, H. Olivares, L. Shi, D. Look, T. M. Gallagher, and S. Perlman.** 2005. A severe acute respiratory syndrome-associated coronavirus-specific protein enhances virulence of an attenuated murine coronavirus. J. Virol. **79:**11335–11342.
34. **Phillips, J. J., M. M. Chua, G. F. Rall, and S. R. Weiss.** 2002. Murine coronavirus spike glycoprotein mediates degree of viral spread, inflammation, and virus-induced immunopathology in the central nervous system. Virology **301:**109–120.
35. **Plotnicky-Gilquin, H., D. Cyblat, J. P. Aubry, Y. Delneste, A. Blaecke, J. Y. Bonnefoy, N. Corvaia, and P. Jeannin.** 2001. Differential effects of parainfluenza virus type 3 on human monocytes and dendritic cells. Virology **285:**82–90.
36. **Ramakrishna, C., S. A. Stohlman, R. D. Atkinson, M. J. Shlomchik, and C. C. Bergmann.** 2002. Mechanisms of central nervous system viral persistence: the critical role of antibody and B cells. J. Immunol. **168:**1204–1211.
37. **Rempel, J. D., S. J. Murray, J. Meisner, and M. J. Buchmeier.** 2004. Differential regulation of innate and adaptive immune responses in viral encephalitis. Virology **318:**381–392.
38. **Schneider-Schaulies, S., I. M. Klagge, and V. ter Meulen.** 2003. Dendritic

cells and measles virus infection. Curr. Top. Microbiol. Immunol. **276:**77–101.
39. **Sevilla, N., S. Kunz, A. Holz, H. Lewicki, D. Homann, H. Yamada, K. P. Campbell, J. C. de La Torre, and M. B. Oldstone.** 2000. Immunosuppression and resultant viral persistence by specific viral targeting of dendritic cells. J. Exp. Med. **192:**1249–1260.
40. **Shaw, E.** 1994. Peptidyl diazomethanes as inhibitors of cysteine and serine proteinases. Methods Enzymol. **244:**649–656.
41. **Simmons, G., D. N. Gosalia, A. J. Rennekamp, J. D. Reeves, S. L. Diamond, and P. Bates.** 2005. Inhibitors of cathepsin L prevent severe acute respiratory syndrome coronavirus entry. Proc. Natl. Acad. Sci. USA **102:**11876–11881.
42. **Stohlman, S. A., C. C. Bergmann, and S. Perlman.** 1998. Mouse hepatitis virus, p. 537–557. *In* R. Ahmed and I. Chen (ed.), Persistent viral infections. John Wiley & Sons, Ltd., New York, N.Y.
43. **Stohlman, S. A., C. C. Bergmann, R. C. van der Veen, and D. R. Hinton.** 1995. Mouse hepatitis virus-specific cytotoxic T lymphocytes protect from lethal infection without eliminating virus from the central nervous system. J. Virol. **69:**684–694.
44. **Trombetta, E. S., M. Ebersold, W. Garrett, M. Pypaert, and I. Mellman.** 2003. Activation of lysosomal function during dendritic cell maturation. Science **299:**1400–1403.
45. **Turner, B. C., E. M. Hemmila, N. Beauchemin, and K. V. Holmes.** 2004. Receptor-dependent coronavirus infection of dendritic cells. J. Virol. **78:**5486–5490.
46. **van Stipdonk, M. J., E. E. Lemmens, and S. P. Schoenberger.** 2001. Naive CTLs require a single brief period of antigenic stimulation for clonal expansion and differentiation. Nat. Immunol. **2:**423–429.
47. **Wu, G. F., and S. Perlman.** 1999. Macrophage infiltration, but not apoptosis, is correlated with immune-mediated demyelination following murine infection with a neurotropic coronavirus. J. Virol. **73:**8771–8780.
48. **Yokomori, K., M. Asanaka, S. A. Stohlman, and M. M. C. Lai.** 1993. A spike protein-dependent cellular factor other than the viral receptor is required for mouse hepatitis virus entry. Virology **196:**45–56.
49. **Yokomori, K., and M. M. C. Lai.** 1991. Mouse hepatitis virus S RNA sequence reveals that nonstructural protein ns4 and ns5a are not essential for murine coronavirus replication. J. Virol. **65:**5605–5608.